An Accurate Lithium-Ion Battery Gas Gauge Using Two-Phase STC Modeling

Hsueh-Chih Yang and Lan-Rong Dung
Department of Electrical and Control Engineering
National Chiao Tung University
Hsinchu, Taiwan, R.O.C.
Email: lennon@faculty.nctu.edu.tw

***Abstract*— The lithium-ion (Li-ion) battery is a time-varying, nonlinear component. Its discharge characteristic is dependent on discharge current, loading change scheme, ambient temperature, and initial state-of-charge (SoC), and hence its remaining time can vary with the discharge operating conditions in a manner of nonlinear relationship. The non-linearity behavior makes the accurate gas-gauge of Li-ion battery very difficult. This paper presents an efficient scheme to simplify the estimation of battery service time with high-degree of accuracy. According to the typical discharge characteristic of Li-ion batteries, we applied a two-phase single-time-constant (STC) model for the gas-gauging strategy and parameterize the discharge operating conditions in terms of the first-phase gradient, the knee voltage, and the second-phase gradient, instead of using complex curve-fitting equations. As shown in the experimental results, the accuracy of predicted remaining time is less than 1% for constant current cases, and 10% for loading change cases.**

I. Introduction

With increasing demands of portable electronics like notebook PCs, cell phones, PDAs, and digital cameras, lithium-ion (Li-ion) and polymer Li-ion batteries are now very popular in the daily lives. The state-of-charge (SoC) of a battery is essential to users and power management policy such like the Advanced Configuration and Power Interface (ACPI) [1]. A battery's SoC is its available capacity expressed as a percentage of its rated capacity. Knowing the amount of energy left in a battery compared with the energy it had when it was new gives the user an indication of how much longer a battery will continue to perform before it is exhausted or needs recharging. However, the discharge behavior of a battery differs from that of a capacitor, and simple equations alone can not determine the SoC. The complicated electrochemical reactions make predicting the battery present remaining capacity and residual service lifetime difficult.

A number of researchers have reported models for predicting the battery remaining capacity or service lifetime. An electrochemical model, DUALFOIL, based on concentrated-solution theory was reported in [2]. It is accurate and general enough to handle a wide range of Li-ion cells, which also provides the extensive use of its companion simulator software [3]. Since electrochemical models are accurate but time consuming in practice. An efficient macromodel for Li-ion batteries was presented in [4], where the battery is modeled by a PSPICE circuit consisting of voltage sources and linear passive elements. [5] approximates a discrete-time circuit model by using VHDL language. Models based on PSPICE and discrete-time VHDL are faster though less accurate. [6] proposed a high-level diffusion-based analytical model. They consider the concentration evolution of the active materials in the battery during a discharge process in a finite region. By identifying the model parameters, the diffusion-based model can predict the battery lifetime given the discharge profile in advance. Researchers also proposed a battery emulator for experiments with battery-aware designs in [7]. The emulator is an intelligent power supply that mimics the behavior of a battery by running a battery simulation program in real-time. It senses the current load and responds by controlling the output voltage as an actual battery would, but it is computationally intensive. A widespread review of battery models and battery-aware issues can be found in [8]. The accurate and fast online estimation of the SoC and the service lifetime of a battery still remains a challenge today.

We aim to develop an accurate and low-complexity gas gauge of a Li-ion battery in practical cases. The gas gauge takes the rate-recovery and rate-capacity effects into account and is capable of predicting the overall discharge curve. We simplified the battery model with accuracy and consider it as a two-phase component as shown in Fig. 2 where an internal resistance R_{int} has two components R_1 and R_2. The discharge curve of a Li-ion battery which was shown in Fig. 3 can be divided into two parts: an exponential voltage decay of the first phase characterized by discharging a fully charged single time constant resistor-capacitor circuit (STC RC circuit) with a long time constant, $\tau = RC$, and a linear change of the second phase characterized by discharging a small capacitor. The exponential decay, $\frac{1}{\tau}e^{\frac{-t}{\tau}}$, can be expanded as a Taylor series, $\frac{1}{\tau}\sum_{n=0}^{\infty}\frac{(\frac{-t}{\tau})^n}{n!}$, where t is time. Since $t \ll \tau$, the first phase, then, was approximated as a linear change. Consequently, applying the approximation combining two straight lines $(L_1 : at + b)$ and $(L_2 : ct + d)$ agrees well with the measured data. We named the intersection "*Knee*" where the voltage was specified as V_K, thereby being aware of the curve entering the second phase. Briefly, we focus attention on statistics of the slopes of two straight lines and V_K to characterize the curve of terminal voltage during constant-current discharge at constant temperature. In addition, the rate-recovery effect or relaxation effect means the battery can recover from its lost efficiency

1-4244-0755-9/07/$20.00 ©2007 IEEE

if given a chance to rest during periods of reduced load. The discharge curve with dynamic current loads can be estimated by carrying out a set of current load tests and cooperating with surface fitting and interpolation techniques.

II. Model Description

The objective of this section is to explain the proposed battery model for the gas-gauging strategy and parameterize the discharge operating conditions.

A. Description of the discharge characteristics

A typical discharge voltage versus time characteristic for a Li-ion battery is given in Fig. 1. Clearly there are four distinct regions; two nonlinear regions (Region 1 and Region 3) and two linear regions (Region 2 and Region 4). From an user point of view the linear regions are the most important. The Region 1, occurring at the start of discharge, typically occupies a small proportion of the total discharge duration. By observing Fig. 1, the discharge curve can be divided into two parts shown in Fig. 3: an exponential voltage decay of the first phase characterized by discharging a fully charged single time constant resistor-capacitor circuit (STC RC circuit) with a long time constant, τ, as described by

$$\tau = RC \tag{1}$$

and a linear change of the second phase characterized by discharging a small capacitor. Therefore, we conclude that a Li-ion battery can be modeled as a two-phase component as shown in Fig. 2 where an internal resistance R_{int} has two components R_1 and R_2. The exponential decay can be expanded as a Taylor series where t is time.

$$\frac{1}{\tau} e^{\frac{-t}{\tau}} = \frac{1}{\tau} \sum_{n=0}^{\infty} \frac{(\frac{-t}{\tau})^n}{n!} \tag{2}$$

Since $t \ll \tau$, the first phase, then, was approximated as a linear change. Consequently, applying the approximation combining two straight lines $(L_1 : at + b)$ and $(L_2 : ct + d)$ agrees well with the measured data. We named the intersection "*Knee*" where the voltage was specified as V_K, thereby being aware of the curve entering the second phase. Briefly, we focus attention on statistics of the slopes of two straight lines and V_K to characterize the curve of terminal voltage during constant-current discharge at constant temperature.

Observing Fig. 4, for the first 800 sec the discharge current was 0.5A. Then, the current load was reduced to 0.4A. Under this condition, the battery recovers its voltage and afterward, discharges in a manner of exhibiting the same behavioral trend of the discharge curve under 0.4A till the end of discharge.

B. Determining model parameters

To validate the proposed equivalent model, the model parameters of a specific battery must be identified experimentally first. We use the battery emulator which was presented in [7] to obtain the discharge curves under a set of constant discharge rates (0.2A, 0.3A, 0.4A, and 0.5A) and a set of two-stage constant discharge rates. The major objective of

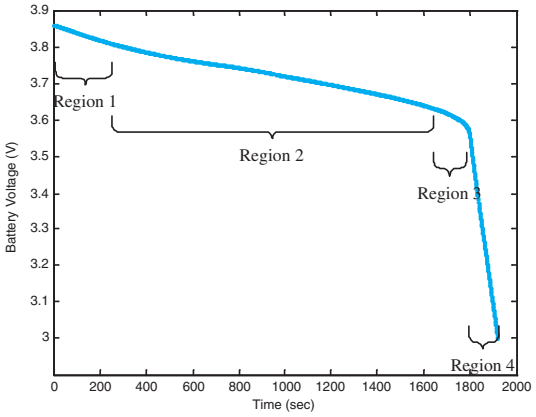

Fig. 1. Typical discharge voltage versus time characteristic illustrating the four regions.

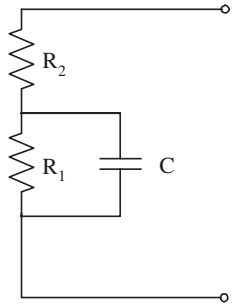

Fig. 2. Equivalent circuit representation of lithium-ion battery.

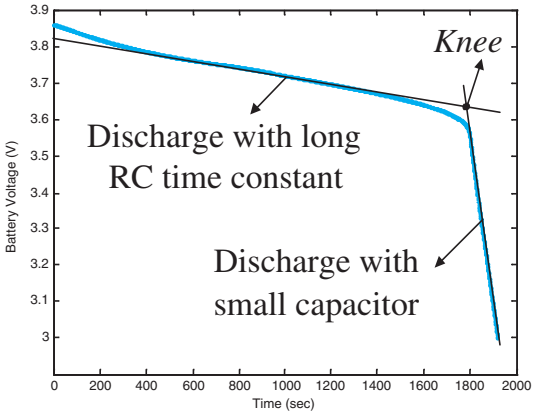

Fig. 3. Typical discharge voltage versus time characteristic divided into two phase with an intersection *Knee*.

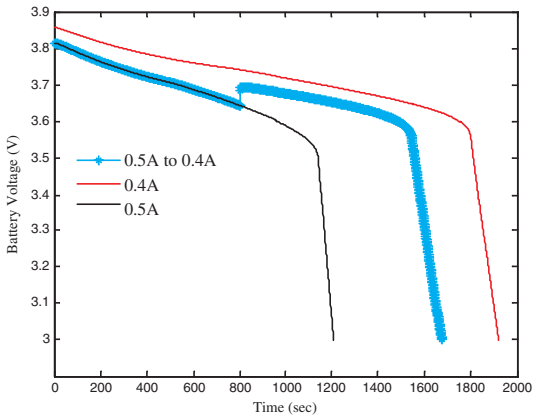

Fig. 4. Rate-recovery effect.

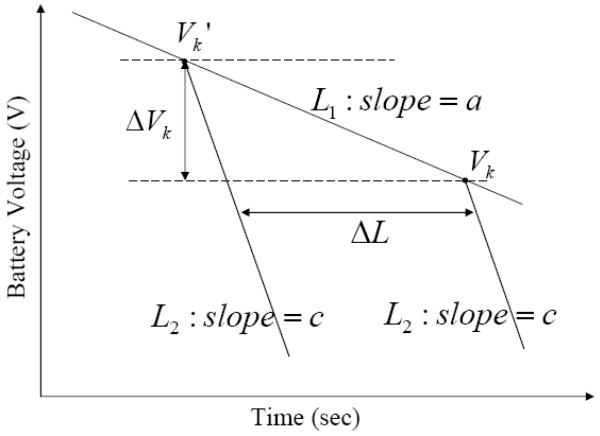

Fig. 7. Geometric representation of sensitivity analysis of ΔV_K.

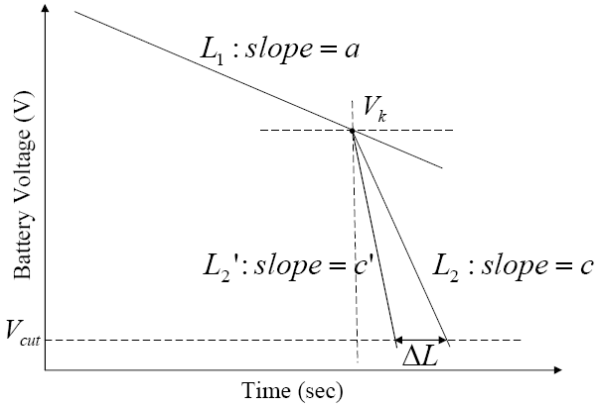

Fig. 8. Geometric representation of sensitivity analysis of Δc.

the simulation is to construct a function which closely fits a discrete set of known data points. Theoretically, all the parameters are multivariable functions of SoC, discharge rate, loading change scheme, and temperature. However, within certain error tolerance, we simplified parameters to be independent or linear functions of discharge rates in a constant-temperature application. We use the fitted data of a set of simulation data of V_K and slopes of L_1 and L_2 under a set of constant discharge rates to estimate discharge curves well for additional constant rates. This is accomplished in Fig. 5 by linearly interpolating between values for V_K and slopes a and c.

C. Sensitivity analysis of model parameters

The sensitivity analysis of model parameters can be performed by using geometric representation as shown in Fig. 7 and 8. The sensitivity analysis presented the effects of the amount of deviation battery service lifetime caused by modeling error. Considering the scenario as shown in Fig. 7, we estimated *Knee* voltage with error, as described by

$$\Delta V_K = V_K' - V_K \tag{3}$$

Therefore, the estimation error of battery service lifetime, ΔL, was derived by

$$\Delta L = \Delta V_K (\frac{1}{|a|} - \frac{1}{|c|}) \tag{4}$$

Approximately, in Eq.(4), the magnitude of ΔV_K is 10^{-4}, and $|a|$ and $|c|$ range between $10^{-5} \sim 10^{-4}$ and $10^{-3} \sim 10^{-2}$ respectively. Consequently, we deduced that the magnitude of ΔL is less than 10^1. In addition, the slope of L_2, c, contributes error to battery service lifetime as well. The magnitude of fitting error of slope c, Δc, as shown in Fig. 6(d), ranges between $10^{-5} \sim 10^{-4}$. For this reason, the fitting error of c will produce service lifetime error less than 10sec by Eq.(5). Moreover, to obtain precise estimation results, the slope of L_1 must be carefully determined, especially when discharge load changes.

$$\Delta L = (V_K - V_{cut})(\frac{1}{|c|} - \frac{1}{|c'|}) = (V_K - V_{cut})(\frac{\Delta c}{cc'}) \tag{5}$$

III. Estimation Algorithm of a Battery's Service Lifetime

A. Notation

The following notation is used in the remainder of this paper.

T_s	sampling period;
C_r	current used to determine rated capacity;
L_r	rated battery service lifetime;
V_{cut}	cut-off voltage;
$V(n)$	present terminal voltage;
$V_K(n)$	present *Knee* voltage;
$I(n)$	present load current;
$T(n)$	present temperature;
$t(n)$	present time;
$m_{L_1}(n)$	present slope of L_1;
$m_{L_2}(n)$	present slope of L_2;
$L(n)$	present estimated battery service lifetime.

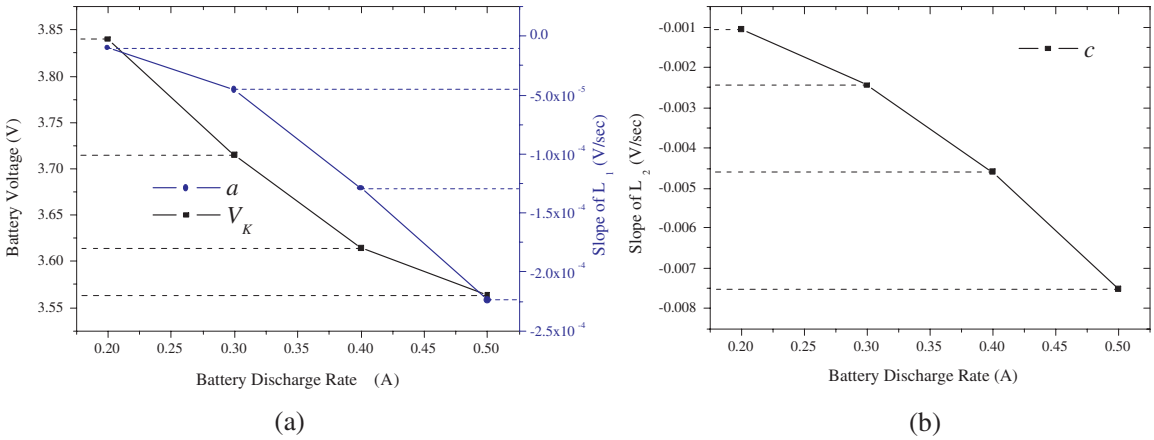

Fig. 5. (a) Parameters V_K and a for a set of constant discharge rates. (b) Parameter c for a set of constant discharge rates.

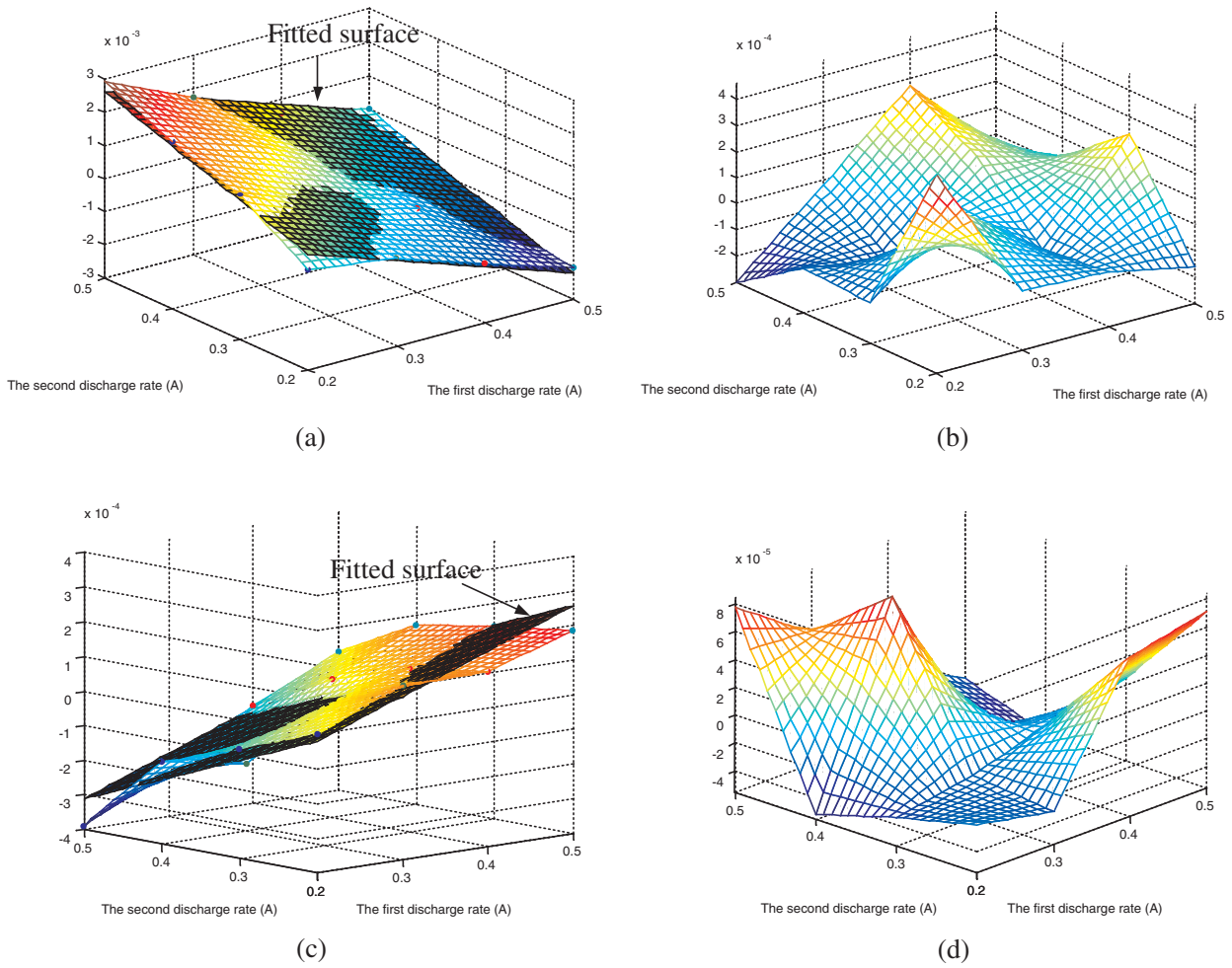

Fig. 6. (a) $S\_V_K(I_1, I_2) = -0.0089I_1 + 0.0072I_2 + 0.0008$, fitted surface of ΔV_K. (b) Fitting error of ΔV_K. (c) $S\_L_2(I_1, I_2) = 10^{-3}(-0.8541I_1 + 0.8369I_2 + 0.3229)$, fitted surface of ΔL_2. (d) Fitting error of ΔL_2.

B. Algorithm description

As explained previously, the discharge characteristic has four distinct regions. The actions carried out during estimating are defined by the region selected. By monitoring the present voltage gradient, $\Delta V(n)$, three kinds of geometric estimation methods can be applied to predict the residual service lifetime by $L(n) - t(n)$ and the remaining capacity by Coulomb counting method accurately. Fig. 9 summarizes the resulting estimation algorithm, which can be divided into several parts. In any of them, the timing functions are generated by interruptions, and every one of them has its own subroutine. Additional characteristics of these parts are briefly reported below.

Measurement:
From the beginning of the algorithm, we monitor the amount of load current, $I(n)$, going out of the battery, the battery's terminal voltage, $V(n)$, and the temperature, $T(n)$, as well as the time, $t(n)$, that passes.

Cut-off Voltage Detected:
Once the algorithm has been started, a very important question is when to finish it. We set a cut-off voltage as the termination condition.

Voltage Slope Calculation:
To obtain the voltage slope of the first phase, the calculation has been made, as described by

$$\Delta V(n) = V(n) - V(n-1) \quad (6)$$

$$m_{L_1}(n) = \frac{\Delta V(n)}{T_s} \quad (7)$$

Slope Gradient:
In Region 1 and Region 3, the slope gradient is nonlinear and gradually smooth, afterwards, entering into linear Region 2 and Region 4 respectively. The present discharge region was determined by two thresholds, TH_1 and TH_2. The slope gradient was defined by

$$gradient = |\Delta V(n) - \Delta V(n-1)| \quad (8)$$

Knee Estimation and *Voltage Slope Estimation:*
As mentioned previously, each specified load current can be used to find the corresponding *Knee* and the slope of L_2 with the data in Fig. 5. V_K and $m_{L_2}(n)$ will not be changed till the load current changes in the proposed algorithm.

$$V_K(n) = V_K(n-1) \quad (9)$$

$$m_{L_2}(n) = m_{L_2}(n-1) \quad (10)$$

Current Load Changed:
When encountering the current measurement noise, we can add one more threshold, TH_3, which is responsible to sensing current loading changes.

Knee Compensation and *Voltage Slope Compensation:*
V_K and $m_{L_2}(n)$ need to be compensated once the load changing has been detected. We compensate V_K and the slope of L_2 for a variable-current discharge load by two fitted surfaces, $S\_V_K(I_1, I_2)$ and $S\_L_2(I_1, I_2)$, shown in Fig. 6 (a) and Fig. 6 (c) respectively. We can use the fitted equations to find the compensation values while load current changes from I_1 to I_2. The compensation methods were formulated by

$$V_K(n) = V_K(n-1) + S\_V_K(I(n-1), I(n)) \quad (11)$$

$$m_{L_2}(n) = m_{L_2}(n-1) + S\_L_2(I(n-1), I(n)) \quad (12)$$

Service Lifetime Estimation (A):
This part of algorithm is used to deal with the scenario that the battery discharges during Region 2. V_K and $m_{L_2}(n)$ should be determined by either estimating or compensating. The present information point, $(t(n), V(n))$, is going to move through the slope direction, $m_{L_1}(n)$, and then we can predict the time when the *Knee* voltage, V_K, will be reached. Subsequently, by using the direction of $m_{L_2}(n)$, $L(n)$ can be determined at the time when the V_{cut} is reached. The formulation was derived as below.

$$L(n) = \frac{V_K(n) - (V(n) - m_{L_1}(n)t(n))}{m_{L_1}(n)} + \frac{V_K(n) - V_{cut}}{m_{L_2}(n)} \quad (13)$$

Service Lifetime Estimation (B):
The scenario that the load current changes during the period when entering into Region 3 and Region 4 has been excluded in the discussion. Consequently, the estimating methods performed in Region 3 and Region 4 are identical. The estimation results do not come with much error.

$$L(n) = t(n) + \frac{V(n) - V_{cut}}{m_{L_2}(n)} \quad (14)$$

Service Lifetime Estimation (C):
The slope in Region 1 degrades rapidly. If we apply *Service Lifetime Estimation (A)* in Region 1, the estimation results will be far away from the truth. Observing that the period of Region 1 is relatively short, we provide a simple equation for reference.

$$L(n) = \frac{I(n)}{C_r} \quad (15)$$

C. Results

The battery emulator, B#, [7] is used to simulate the battery voltage characteristics for comparison. B# is a programmable power supply that emulates the behavior of a battery. It measures the current load, calls a battery simulation program to compute the voltage in real time, and controls a linear regulator to mimic the voltage output of a battery. We perform a series of simulations with dynamic current load by modifying the parameters as shown in Fig. 10. The column labelled "err%" in Table I refers to the percentage of the difference between the battery service lifetime obtained by using the proposed gas gauge hardware and the B# emulator. As shown in the comparison results, the accuracy of predicted lifetime is less than 10% for loading change cases.

IV. Conclusion

We have developed an accurate and low-complexity gas gauge for Li-Ion battery. The gas gauge takes the rate-recovery and rate-capacity effects into account and is able to predict the discharge time. The battery is modeled as a two-phase STC network. As shown in the results, the proposed gas gauge can

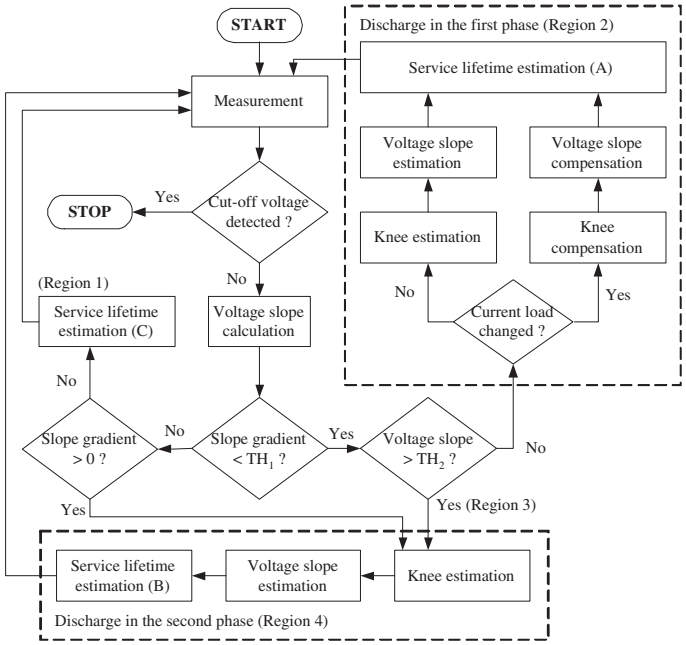

Fig. 9. Flowchart of estimating present remaining capacity and residual service lifetime.

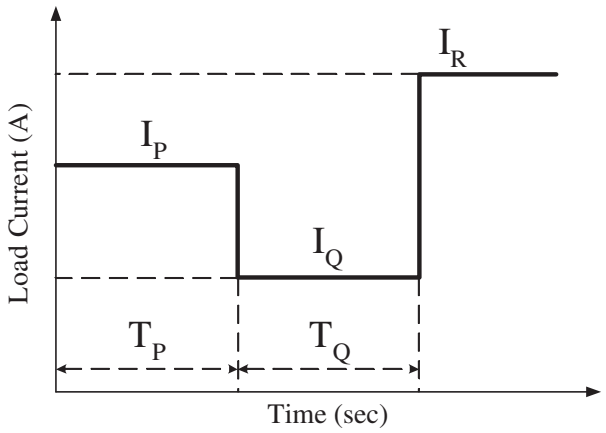

Fig. 10. Dynamic load current profile example.

estimate the remaining discharge time with high degree of accuracy.

TABLE I
COMPARISON RESULTS.

T_P	T_Q	I_P	I_Q	I_R	[7](sec)	proposed(sec)	err%
200	300	0.8	0.4	0.4	1741	1764	1.31
300	300	0.8	0.4	0.4	1624	1532	-6.71
100	300	0.8	0.5	0.5	1151	1128	-1.98
400	300	0.8	0.5	0.5	912	838	-8.16
300	300	0.8	0.6	0.6	724	703	-2.90
100	300	0.6	0.4	0.4	1881	1927	2.44
500	300	0.6	0.4	0.4	1649	1490	-9.67
300	300	0.6	0.8	0.8	562	557	-0.92
200	300	0.4	0.5	0.5	1250	1172	-6.21
600	300	0.4	0.5	0.5	1347	1344	-0.23
700	300	0.4	0.6	0.6	1113	1159	4.17
200	300	0.5	0.4	0.4	1879	1855	-1.30
600	300	0.5	0.4	0.4	1760	1670	-5.13
200	300	0.5	0.8	0.8	557	524	-5.87
400	300	0.5	0.8	0.8	648	659	1.76
200	300	0.2	0.4	0.4	2001	2059	2.92
600	300	0.2	0.4	0.4	2187	2259	3.27
100	300	0.2	0.8	0.8	553	524	-5.22
400	300	0.2	0.8	0.8	790	782	-1.06
400	400	0.5	0.4	0.3	3265	3197	-2.08
500	400	0.5	0.4	0.3	3196	3275	2.48
500	500	0.5	0.4	0.3	3147	3264	3.72

REFERENCES

[1] (Oct. 2006). *Advanced Configuration and Power Interface Specification, Revision 3.0b*. [Online]. Available: http://www.acpi.info/spec.htm

[2] T.F. Fuller, M. Doyle, and J. Newman, "Modeling of galvanostatic charge and discharge of lithium-ion insertion cells," *J. Electrochem. Soc.*, vol. 141, no. 1, pp. 1–9, Jan. 1994.

[3] (May 2005). *FORTRAN Programs for Simulation of Electrochemical Systems*. [Online]. Available: http://www.cchem.berkeley.edu/ jsngrp/fortran.html

[4] S. Gold, "A PSPICE macromodel for lithium-ion batteries," in *Proceedings of the 12th Battery Conference*, pp. 9–15, 1997.

[5] L. Benini, "Discrete-time battery models for system-level low-power design," *IEEE Trans. Very Large Scale Integr. (VLSI) Syst.*, vol. 9, no. 5, pp. 630–640, Oct. 2001.

[6] D. Rakhmatov and S.B.K. Vrudhula, "An analytical high-level battery model for use in energy management of portable electronic systems," in *Proc. IEEE Int. Conf. Comput.-Aided Des.*, pp. 488–493, Nov. 2001.

[7] C. Park, and J. Liu, and P.H. Chou, "B#: a battery emulator and power profiling instrument," *The International Symposium on Low Power Electronics and Design (ISLPED)*, pp. 288–293, Aug. 2003.

[8] R. Casas and O. Casas, "Battery sensing for energy-aware system design," Computer, vol. 38, no. 11, pp. 48–54, Nov. 2005.